

VIII-II-1. Project Research

Project 8

Y. Kawabata

Research Reactor Institute, Kyoto University

OBJECTIVES AND ALLOTTED RESEARCH SUBJECTS :

The aim of this project research is the development of neutron optical devices and its application.

ARS-1 Development of milli-focus X-ray CT system

ARS-2 Observation of water movement in grafted stems of tomato seedlings

ARS-3 Visualization of welding defect in a heatsink for an accelerator of switching power supply

ARS-4 Observation of magnetization in polarizing supermirror by neutron magnetic phase contrast imaging

ARS-5 Improvement of layer structure for low-m supermirror fabricated on an ordinary silicon substrate

ARS-6 Development of high frequency resonance spin flipper with dipole magnet

MAIN RESULTS AND THE CONTENTS OF THIS REPORT :

S. Tokumoto et al. (ARS-1) have developed a milli-focus X-ray CT system. It is possible to measure internal shapes with the spatial resolution of 50 μ m. It is much better than that of the industrial x-ray CT. This milli-focus CT is the 3rd generation type by driven ROTETE-ROTATE. CT volume data image of resin spray can distinguish the different materials with the images of two parts, which are a spray head (polypropylene(PP)) and a jet orifice (high density polyethylene).

U. Matsushima et al., (ARS-2) discussed about the observation of water movement in grafted stems of tomato seedlings. Water flow of different stage of grafted tomatoes and will be studied. Velocity of water flow would indicate the process of development of a tissue at each development stage. They will also improve water flow calculation method using D₂O tracer.

N. Takenaka et al. (ARS-3) has visualized the welding defect in a heatsink of switching power supply for an accelerator by using neutron CT. The heatsink is made of copper, and the part about 3cm from the edge was cut for observation. It was put on an automatic rotating stage, and a picture was taken every 1.8 degree. A computed tomography was carried out using the 100 pictures which correspond to 180 degree. The visualized images by neu-

tron radiography shows the water channel in the heatsink. The vertical water channel was drilled from the top, and the plug was brazed. Therefore, the water may leak from the brazing part. From the original pictures, CT was carried out. The brazing part was observed more brightly. The brazing shape must be circle for preventing the water leakage. However, the brazing shapes were not completely circle at some horizontal positions, and defective area can be observed. Therefore, it can be concluded that the defective causes the water leakage, and the improvement is required.

S. Tasaki et al. (ARS-4) observed the magnetization in a polarizing supermirror by neutron magnetic phase contrast imaging. They measured a 5Q-polarizing supermirror, fabricated with ion beam sputtering in KURRI. The supermirror consists of Fe, and Ge, each of which is sandwiched by thin layers of Si. Total thickness of Fe is 6.4 μ m. Using neutron spin phase contrast imaging, magnetization in the polarizing supermirror is clearly observed.

M. Hino et al. (ARS-5) improved the layer for low-m supermirror fabricated on an ordinary silicon substrate. They have succeeded in fabricating m=6 supermirrors using ion beam sputtering (IBS) technique at KURRI. The measured neutron reflectivities were well reproduced by the simple interface roughness model given in Debye-Waller factor. The surface roughness of ordinary substrate, for example commercial silicon wafer and float glass, is almost larger than 0.4 nm in rms (root-mean-square). They realized almost theoretical reflectivity limit of m=2.9 NiC/Ti supermirror by ion beam sputtering technique. It is effective for high reflectivity low-m supermirror deposited on an ordinary substrate to increase the number of layer.

M. Kitaguchi et al. (ARS-6) are developing a high frequency resonance spin flipper for neutron resonance spin echo including MIEZE. They confirmed the stability and the smoothness of the magnetic fields provided by the dipole magnets. MIEZE spectrometer is under final process to practical use. Various sample environments can be installed because no devices are required after the sample in the setup of MIEZE. Some measurements including magnetic scattering has started in order to demonstrate the feasibility of the MIEZE spectrometer.

S. Tokumoto and S. Katsunori

System Division, Industrial Technology Center of Wakayama Prefecture

INTRODUCTION: Though we can measure internal shapes of various objects by using industrial X-ray CT in the industrial technology center of Wakayama prefecture, the image resolution of this system is not enough for internal shapes of small objects. Therefore we have developed milli-focus X-ray CT shown in Fig.1 to measure small and non-metal objects with high accuracy. Development of the fusion of X-ray CT and Neutron CT is our next target to collaborate with Research reactor institute, Kyoto university.

CHARACTERISTICS OF NEW X-RAY CT SYSTEM: Basic specs of the developed milli-focus X-ray CT are shown in Table.1. It is possible to measure internal shapes by using the milli-focus CT that have spatial resolution of 50 μ m. It is much better than that of the industrial x-ray CT. The milli-focus CT is the 3rd generation type by driven ROTETE-ROTATE.

Table.1

Scanning Method	The third generation method
X-rays Output	50kV 1mA
Detector Area	120 \times 120[mm]
Spatial Resolution	MIN each 0.05[mm]
Scan Speed	2min(Spatial resolution 0.2[mm]) 4min(Spatial resolution 0.1[mm]) 8min(2min(Spatial resolution 0.05[mm])) (Rough estimate)

CT volume data image of resin spray measured by the milli-focus CT is shown in Fig.2. The size of this spray is 24 \times 20 \times 26[mm]. We can improve the accuracy of the milli-focus CT by dimension measurement of virtual CMM (Coordinate Measuring Machine) that has been added to volume rendering software. The material of this spray head is a polypropylene(PP) and that of jet orifice is high density polyethylene. We can distinguish the different materials with the images of these two parts. CT volume data image of cotton work glove resin measured by the milli-focus CT is also shown in Fig.3. We can recognize knitted loops of cotton work glove from this figure.

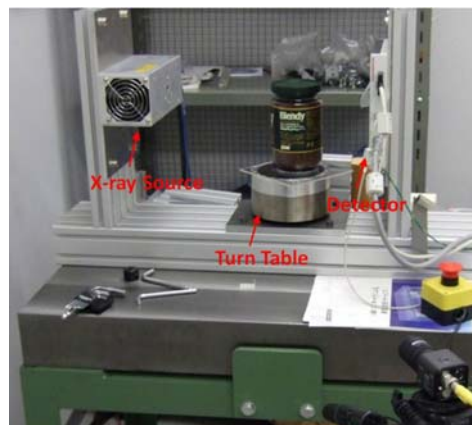


Fig.1. Milli-focus X-ray CT System.

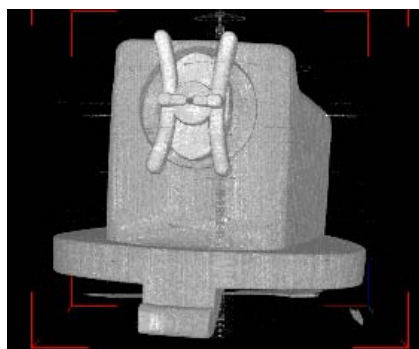


Fig. 2. X-ray CT volume data (resin spray).

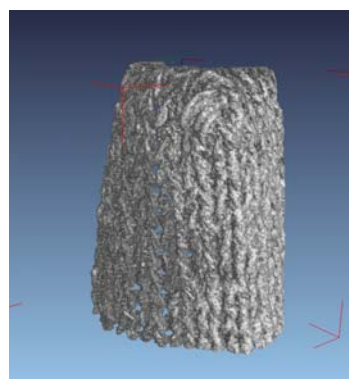


Fig. 3. X-ray CT volume data (cotton work glove).

PR8-2 Observation of Water Movement in Grafted Stems of Tomato Seedlings

U. Matsushima, M. Hino¹, M. Kitaguchi¹ and Y. Kawabata¹

Faculty of Agriculture, Iwate University

¹*Research Reactor Institute, Kyoto University*

INTRODUCTION: Water transport in plants is one of the most important factors for the life, because it guarantees plants photosynthesis the basic process for live on earth. Water flow also regulates various plant physiological phenomena. Using neutron radiography, development of grafted seedling tissues will be observed. Grafting is a method to transplant e. g. weakly growing but effectively fruiting shoots (scion) to strong root stocks. The grafting process is difficult to investigate by yet existing destructive methods. However it is very important to know grafting process to rise the success rate. Water flow in grafted stems of different developing stages will be clarified by this observation. The knowledge would help to develop new effective grafting methods for farmers. Water flow visualization using neutron radiography with D₂O tracer was suitable tool to investigate water movement in the grafting seedlings [1].

EXPERIMENTAL PLAN: The objectives of this experiment are to observe development of grafted tomato tissues. Water flow of different stage of grafted tomatoes and will be studied (Figure 1). Velocity of water flow would indicate the process of development of a tissue at each development stage. We will also improve water flow calculation method using D₂O tracer. Block matching that is one of optical flow algorithms was applied to calculate water flow from sequential neutron radiography images that show water uptake [2]. After a grafting process, a grafted tissue has complex vessel arrangement because of the connection of two different plants. The anatomy should relate to water flow in the stem. Development of the grafted tissue and vessels also should be observed using other microscopic measurement, because resolution of neutron radiography is not enough to see the detail.

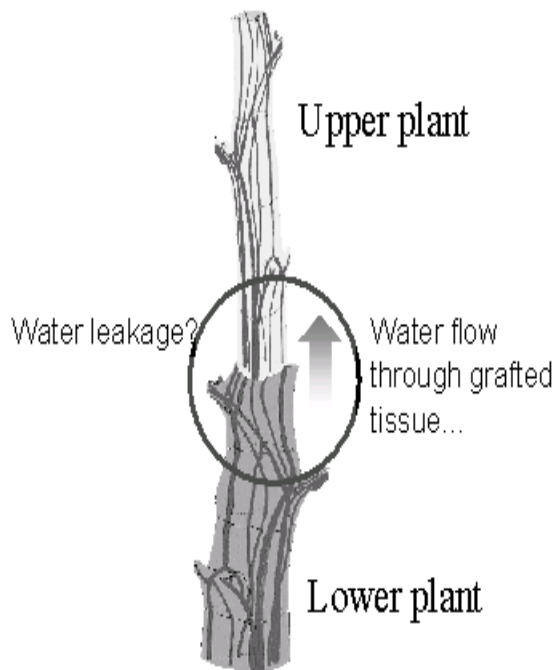


Fig. 1. Schematic diagram of grafted place of upper and lower plants.

REFERENCES:

- [1] U. Matsushima, W. B. Herppich, N. Kardjilov and A. Hilger: BENSIC Exp. Rep. 2007, 183 (2008).
- [2] U. Matsushima, W. B. Herppich, N. Kardjilov, W. Graf, A. Hilger and I. Manke, Nucl. Instr. and Meth. A, in press (2009).

Visualization of Welding Defect in a Heatsink for an Accelerator of Switching Power Supply

N. Takenaka, H. Murakawa, M. Kawai¹, Y. Kawabata² and C.M. Sim³

Department of Mechanical Eng., Kobe University

¹*Institute of Materials Structure Science, KEK*

²*Institute of Research Reactor, Kyoto University*

³*Korean Atomic Energy Institute*

INTRODUCTION: Pulse voltage changes in a digital accelerator to accelerate the ion beam. Therefore, high-speed switching power supply is one of the important systems. It requires high repetition frequency (~MHz), high power (~kW) and low power loss. In particular, cooling system of the power supply affects on the stable operation of the system. For cooling the power supply, water-cooled heatsink as shown in Fig.1 is used. The heatsink was drilled for water channel, and silver brazed the plug. However, water leak was confirmed from the brazing part. In order to observe the defect, neutron CT was carried out at HANARO in KAERI.

EXPERIMENTAL APPERATUS: The heatsink is made of copper, and the about 3cm from the edge was cut for observation. It was put on an automatic rotating stage, and a picture was taken every 1.8 degree (Fig.1). A computed tomography was carried out using the 100 pictures which correspond to 180 degree.

RESULTS AND DISCUSSION: Fig.2 shows examples of the visualized images of the heatsink. Water channel

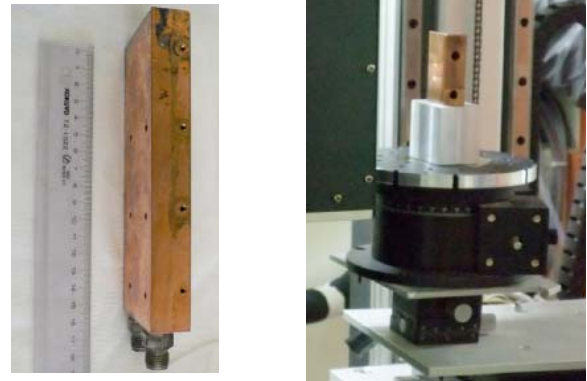


Fig. 1. Water-cooled heatsink.

can be observed in the heatsink. The vertical water channel was drilled from the top, and the plug was brazed. Therefore, the water may leak from the brazing part. From the original pictures, CT was carried out as shown in Fig.3. The brazing part was observed more brightly. The brazing shape must be circle for preventing the water leakage. However, the brazing shapes were not completely circle at some horizontal positions, and defective area can be observed. Therefore, it can be concluded that the defective causes the water leakage, and the improvement is required.

CONCLUSIONS: Heatsink of a power supply was observed by using neutron CT. From the result, defective of silver welding was confirmed, and the improvement of the heatsink is required

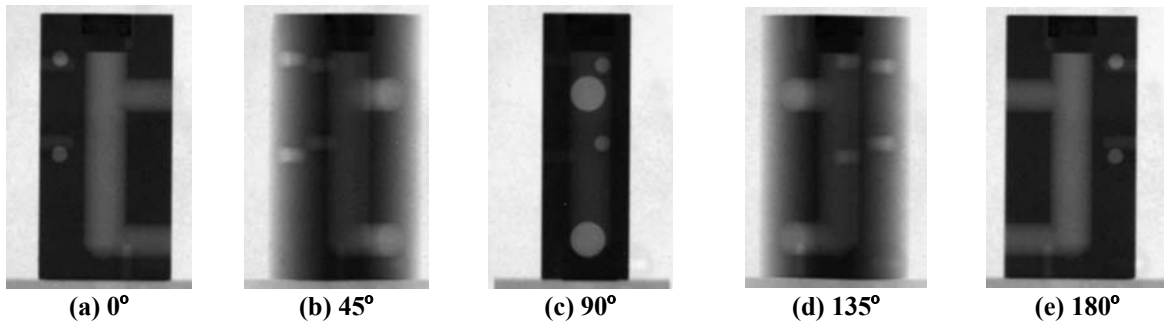


Fig. 2. Original images.

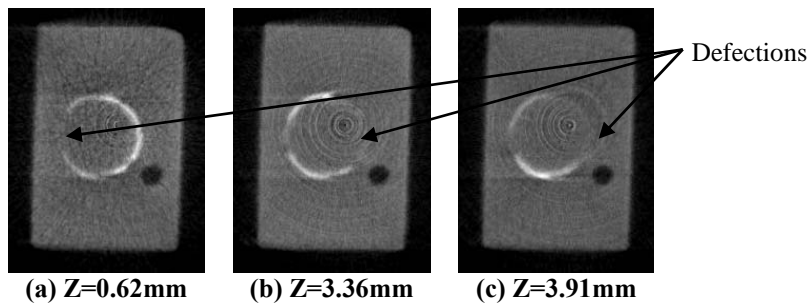


Fig. 3. CT reconstructed images.

S. Tasaki, M. Kageyama, Y. Abe and M.Hino¹

Graduate School of Science, Kyoto University
¹Research Reactor Institute, Kyoto University

INTRODUCTION: Neutron spin phase contrast (NSPC) imaging is a method to visualize the magnetic field integral along the trajectory of neutron. The principle of NSPC is to measure additional phase difference between spin eigen states of Larmor precessing neutron, by means of neutron spin interferometry. In NSPC imaging, neutron intensity changes sinusoidally, via the phase difference of incident neutron. When magnetic field exist on the way of neutron, the sinusoidal curve is shifted, and the shift is proportional to the magnetic field integral. Moreover, the contrast (visibility) of the sinusoidal curve may change depending on the homogeneity and direction of the magnetic field.

In the present study, we measure a 5Q-polarizing supermirror, fabricated with ion beam sputtering in Research Reactor Institute of Kyoto University. The supermirror consists of Fe, and Ge, each of which is sandwiched by thin layers of Si. Total thickness of Fe is 6.4 μ m.

EXPERIMENTS: Neutron experiments were performed at C3-1-2-2 beam port of JRR-3M in JAEA. Wavelength of the neutron beam is 0.88nm ($\delta\lambda/\lambda=2.7\%$), available beam size is 2mm in width and 30mm in height. As the neutron detector, we adopted an Imaging Plate (IP), because spatial resolution of IP (50 μ m) is much better than other detectors.

The neutron intensity for each phase of incident neutron is recorded sequentially on the different position in the IP. The measurements were performed under two sample conditions: *i.e.* before and after magnetization. The sample had been kept in dry container without any magnetic field for months before the first measurement. After the measurement, the magnetic field of 580Gauss was applied to the sample for one minute to magnetize the sample, and then the second measurement was performed.

In NSPC measurement, a weak magnetic field (8.6Gauss) is applied around the sample, which has little effect on the sample magnetization.

RESULTS: The sample image, phase image and visibility image are shown in Fig.1. Figure 1 (a) shows the whole sample and square in the figure represents the beam irradiated area. Figure 1 (b) and (c) show the phase image (b) before and (c) after magnetization, respectively. In Fig.1 (b), there exist unmagnetized area, which is clearly disappeared after magnetization. Figure 1 (d) and (e) show the visibility image (d) before and (e) after magnetization, respectively. In Fig.1 (d), there

exists definite area with low visibility around the center of the sample, which corresponds to the low phase area in (b). This area, however, disappears after magnetization.

CONCLUSION: Using NSPC imaging, magnetization in the polarizing supermirror is clearly observed. This method can be powerful tool for developing magnetic mirrors.

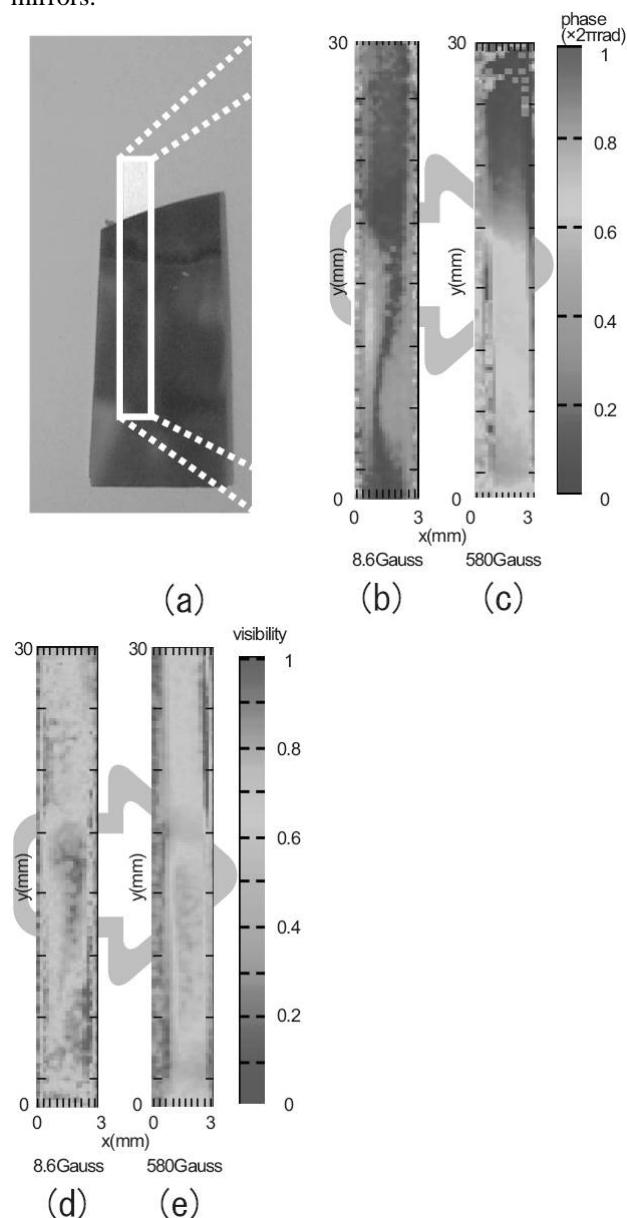


Fig. 1. (a) Photograph of whole sample. (b) Phase image before magnetization. (c) Phase image after magnetization. (d) Visibility image before magnetization. (e) Visibility image after magnetization.

PR8-5 Improvement of Layer Structure for Low- m Supermirror Fabricated on an Ordinary Silicon Substrate

M. Hino, M. Kitaguchi, Y. Kawabata, N. Achiwa¹ and S. Tasaki²

Research Reactor Institute, Kyoto University

¹Grad. School of Science, Osaka University,

²Department of Nucl. Eng., Kyoto University

INTRODUCTION: Supermirror with large- m are desirable to enlarge utilization efficiency for neutron scattering experiments and it is also very important to fabricate high reflectivity supermirror even in low- m (Here m is a maximum critical angle of the mirror in unit of critical angle of nickel).

EXPERIMENTS: We have succeeded in fabricating $m=6$ supermirrors using ion beam sputtering (IBS) technique at KURRI. The measured neutron reflectivities were well reproduced by the simple interface roughness model given in Debye-Waller factor. The surface roughness of ordinary substrate, for example commercial silicon wafer and float glass, is almost larger than 0.4 nm in rms (root-mean-square).

In the Debye-Waller model, a reflectivity (R_{DW}) with the rms interface roughness σ is given by $R_{DW} = R_{cal} \exp(-\sigma^2 Q^2)$, where R_{cal} is the theoretical reflectivity, $Q = 4\pi \sin\theta / \lambda$, θ and λ are the glancing angle and wavelength of incident neutron beam, respectively. Figure 2(a) shows theoretical reflectivity of $m=3$ supermirror with roughness ($\sigma=0.4$ nm). The R_{cal} calculated including the incoherent and absorption cross section of Ni and Ti. The algorithm for supermirror design is based on ref.[2] and the incident neutron wavelength resolution is 2.7 % in order to compare experimental data. The proper number of layer for $m=3$ Ni/Ti supermirror is less than 500 since it is not effective for improvement of reflectivity to increase number of layer in which is larger than 400. The maximum reflectivity of $m=3$ Ni/Ti supermirror without roughness ($\sigma=0$) at the critical angle is 0.95 and that with roughness ($\sigma=0.4$ nm) is smaller than 0.9. The theoretical proper number of layer is less than 500 although nuclear potential value of the NiC layer is 5% smaller than that of nominal Ni layer. We fabricated $m=3$ supermirror in which number of layer is 650 in order to estimate the effect of number of layer. We used an ordinary silicon wafer in which surface roughness is about 0.4 nm. Figure 2(b) shows measured and theoretical reflectivity

by the $m=3$ NiC/Ti supermirror. As shown in the inset of Fig.2.(b), the measured reflectivity at $m < 2.8$ was much better than the expected theoretical lines with $\sigma=0.3$ nm. It was well reproduced by the theoretical line with ideal smooth layer structure in which surface and interface roughness is nothing or very little ($\sigma < 0.1$). We realized almost theoretical reflectivity limit of $m=2.9$ NiC/Ti supermirror by ion beam sputtering technique. It is effective for high reflectivity low- m supermirror deposited on an ordinary substrate to increase the number of layer. It is also useful for realization of small d-spacing monochromator with high reflectivity.

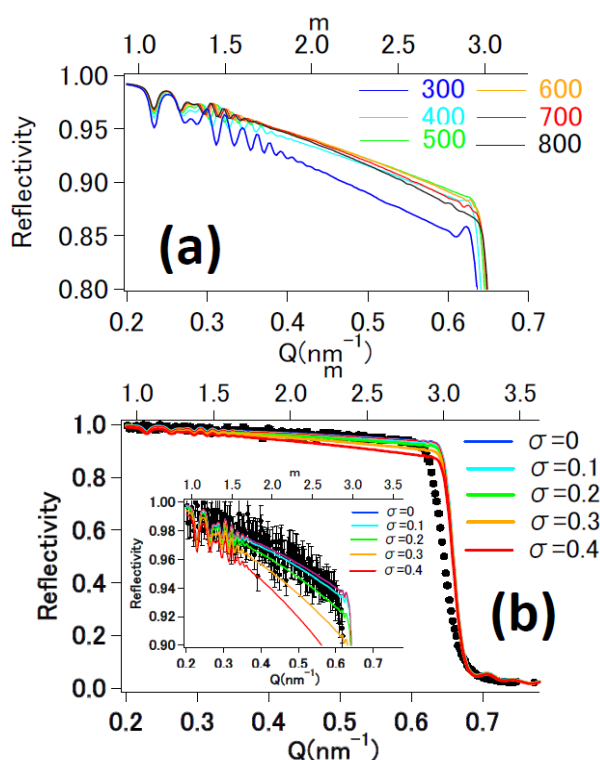


Fig. 1. (a) Numerical simulation of reflectivities on $m=3$ supermirrors in which number of layers are from 300 to 800 with $\sigma=0.4$ nm, respectively. (c) Measured reflectivity of $m=2.9$ supermirror in which number of layers is 650. The solid lines indicate theoretical ones with $\sigma=0, 0.1, 0.2, 0.3$ and 0.4 nm. The inset is enlarged at high reflectivity ($R > 0.9$)[2].

REFERENCES:

- [1] T.Ebisawa, *et al.*, J.Nucl. Sci. Technol., **16** (1979) 647.
- [2] M.Hino, *et al.*, Nucl.Inst.Meth. A, **600** (2009) 207.

PR8-6 Development of High Frequency Resonance Spin Flipper with Dipole Magnet

M. Kitaguchi, M. Hino, Y. Kawabata, S. Tasaki¹, R. Maruyama² and T. Ebisawa²

Research Reactor Institute, Kyoto University,

¹Department of Nuclear Engineering, Kyoto University

²JAEA

INTRODUCTION: Neutron spin echo (NSE) is one of the techniques with the highest energy resolution for quasi-elastic scattering by measuring rotation of the neutron spin[1]. In neutron resonance spin echo (NRSE), two resonance spin flippers (RSFs) replace a homogeneous static magnetic field for spin precession in the conventional NSE[2]. An RSF, which flips the spin of a neutron by exchanging energy between the neutron and an oscillating magnetic field, gives the difference of wavenumber between up- and down-spin components of the neutron. The relative phase between the two spin components, which is equivalent to spin rotation, is provided by the difference of wavenumber in the area between the RSFs. A RSF consists of a static magnetic field and an oscillating magnetic field. The static field is proportional to the frequency of the oscillating field. The energy resolution of NRSE spectrometer is proportional to the frequency of the oscillating field. The static field of 17mT is required for the frequency of 500kHz. It was quite difficult to provide the strong static field corresponding to the high frequency up to 500kHz by using air-core coils.

EXPERIMENTS: New type of RSF has been developed by using dipole magnet with iron poles for the static magnetic field (figure 1). It could provide strong magnetic field with less current, however, magnetic flux leak and its surface was not well-defined. The gap between the two iron poles had the height of 150mm. The dipole magnet had the uniform magnetic field with the center area of 15mm width, 15mm height and 50mm long. The uniformity was less than 10%. About 20mT was measured at the center of the uniform field area with the current of 8A. The magnetic field was quite stable by using the regulated power supply. Temperature of the coil was also stable for the magnetic field which was less than 20mT without any additional cooling system. The return field was enclosed by iron yoke around the magnet well. Additionally there were small iron parts to reduce the extending of the magnetic flux in the beam area before and after the RSF. Test experiments to observe MIEZE signals with high frequency by using the new RSFs have been performed using the cold neutron beam line MINE1 at JRR-3 reactor at JAEA. The beam had the wavelength of 0.81nm and the bandwidth of about 10%. The frequency of the first RSF was 300kHz and that of the second RSF was 600kHz. Figure 2 shows the MIEZE signal with normalization of the detector efficiency. Neutron counts modulated according to the phase of the oscillating field of the RSFs. The contrast of the signal was 0.58.

RESULTS: We confirmed the stability and the smoothness of the magnetic fields provided by the dipole magnets. MIEZE spectrometer is under final process to practical use. Various sample environments can be installed because no devices are required after the sample in the setup of MIEZE. Some measurements including magnetic scattering has started in order to demonstrate the feasibility of the MIEZE spectrometer. We are continuing to develop RSF with much higher frequency for NRSE spectrometer with high resolution. We will utilize the new system including the new RSFs for the development of a neutron spin echo spectrometer at J-PARC[3].



Fig. 1. RSF with dipole magnet with iron pole.

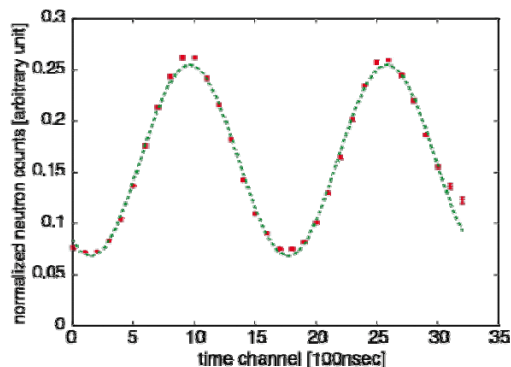


Fig. 2. MIEZE signal with 600kHz.

REFERENCES:

- [1] F. Mezei, Z. Phys., **255** (1972) 146.
- [2] R. Gähler, R. Golub, Z. Phys. B, **65** (1987) 43.
- [3] Y. Kawabata, *et. al.*, Nucl. Instrum. Meth. A, **574** (2006) 1122.